76 KSME Journal, Vol. 7, No. 1, pp. 76~85, 1993

Tracer of Complex Movement by Using Five Optical Line Detectors and Fifth-Order Cross-Correlation Analysis

Kyung Y. Jhang*, Yuji Saito and Takuso Sato****

(Received August 10, 1992)

A new method to detect the trace of complex movement of vehicle by using five optical line detectors and fifth-order cross-correlation analysis is proposed. In this method, the curvature and center coordinates of trace segment can be estimated simultaneously together with the velocity of the vehicle's motion. Hence the trace of the vehicle in a fixed measuring time interval can be detected as a circular arc and the whole trace is reconstructed as the connection of these arcs. To confirm the usefulness of the proposed method, an actual measurement system has been constructed and experiments using the sham road of which movement was controlled have been carried out. The details of the principle, system construction and the results are shown.

Key Words: High-Order Correlation Analysis, Line Detector, Movement Detection, Tracer

1. Introduction

Trace measurement is required not only to record the trace of vehicle but also to detect the breaking away of the automatically or remotely controlled vehichle from the desired course and so to confirm whether the vehicle has been moved exactly according to the control or not.

The most commonly used method for the trace measurement is to iterate the measurement of velocity and steering angle in short time intervals to reconstruct the trace as a sequence of straight lines. There have been two ways to measure velocity and steering angle: one is the contact or direct method and another is the without contact or indirect method. The example of the former one are the tachometer and the steering angle detector. In the direct method, however, the mechanical contact error, for instance, may results in the velocity detecting error dur to the slip between tires and the road or steering angle deviation due to the pressure unbalance between right and left tires. To avoid these defects, serveral indirect or without contact methods have been developed. Among them, second-order cross-correlation method (Idogawa, 1975), spatial filter (Kobayashi, 1980), Doppler velocimetry (Mason, 1979), etc. are used for velocity detection, and as for the steering angle detection, several kinds of gyro scopes have been developed (Bergh, 1984 and Konno, 1989).

The basis of most of the above method, however, is to approximate the trace as a combinatioin of straight lines, so it is difficult to detect the trace of actual complex movement with good accuracy. Moreover, it needs the combination of the two measurement systems, one for the velocity detection and another for the steering angle detection.

In this paper, a new method to measure the trace of a complex movement with a single mea-

* Hanyang Univ., Dept. of Precision Mechanical Engineering, Haengdang-dong 17, Seongdong-gu, Seoul 133-791, Korea

** The Graduate School at Nagatsuta, Tokyo Institute of Technology, 4259 Nagatsuta, Midori-ku, Yokohama-shi 227, Japan

surement system by using five optical line detectors mounted on the vehicle and fifth-order cross-correlation analysis of the detected signals is proposed. It is an extension of the second-order cross-correlation method which measures the mean velocity by using second-order correlation analysis for the estimation of the time delay between two detectors separated by a finite distance. In the new system, however, five line detectors and fifth-order cross-correlation analysis are used, so that the curvature and its center coordinates as well as the velocity of the vehicle can be detected simultaneously. The trace that the vehicle has moved during the fixed time interval can be estimated as a circular arc and the whole trace is reconstructed sequencially by connecting these arcs. Thus this method may have significant advantages over the previous straight line approximation method in the accuracy especially when the motion of the vehicle is complex and the implementation to practical system is also easy.

To confirm the usefulness of the proposed method, a prototype measurement system has been constructed and preliminary experiments using the sham road have been carried out, where we moved the sham road instead of directly moving the vehicle. As the sham road, monochrome photographs of the real road and the plate with the randomly distributed white and black pattern on the surface have been used.

The details of the principle, required signal processings, including the fifth-order cross-correlation analysis, and the experimental results are shown in the following.

2. Principles

Figure 1 illustrates the turning motion of a vehicle with angular velocity ω_R, where the optical line detectors are mounted on the vehicle. The point o_R is the arbitrarily established reference point to represent the motion of the vehicle as the trace of this point. In the present case, it is set conveniently at the center of the group of line detectors. Our purpose is to approximate the trace

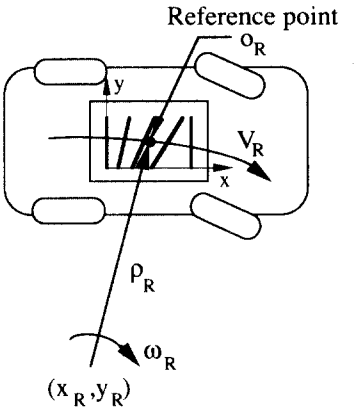

Fig. 1 Parameters to identify the trace of vehicle moving according to the circular arc

of this reference point by a circular arc by determining center coordinates (x_R, y_R), radius of curvature ρ_R and velocty V_R. The methodology to measure these parameters will be described in sections A and B. By repeating this measurement and sequentially connecting the detected arcs, the whole trace is reconstructed. This reconstruction process is described in the section C.

2.1 Trace detection as the approximated circular arc

In order to obtain the four parameters which determine the trace in a segment, that is, coordinates of center, x_R, y_R, radius of curvature ρ_R, and velocty V_R, five optional line detectors, denoted $LD_1 \sim LD_5$ are used, and fifth-order crosscorrelation analysis is applied to the detected signals.

The optical line detectors are arranged so that they intersect the x axis at $x=0$, $x=x_1$, $x=x_2$, $x=x_3$ and $x=x_4$, respectively where $0<x_1<x_2<x_3<x_4$, as shown in Fig. 2. In this arrangement, the line detectors LD_1 and LD_5 are put so that they are parallel to each other. The other line detectors, LD_2, LD_3 and LD_4, however, are put on the lines given by the equation $y=(x-x_1)\tan\beta$, $y=(x-x_2)\tan\gamma$ and $y=(x-x_3)\tan\psi$, respectively, where $0<\Psi<\gamma<\beta<\pi/2$. Moreover, the five line detectors are arranged so that do not intersect each other within the detection area.

The line detectors are used to observe the

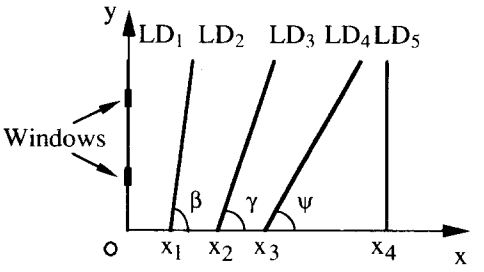

Fig. 2 Arrangement of optical line detectors with two windows on the first detector

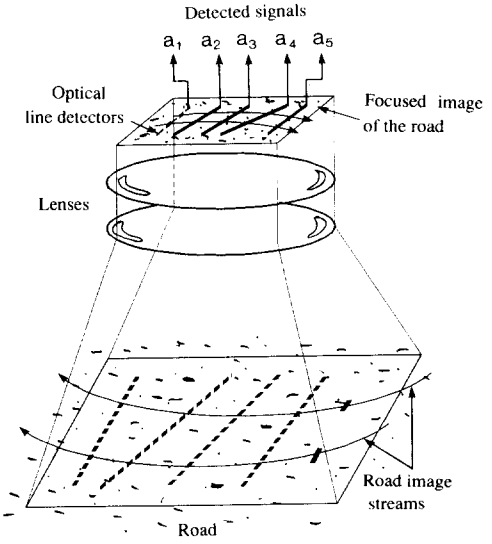

Fig. 3 Focusing of the road image pattern and its detection by optical line detectors

movement of corresponding lines on the road surface as the intensity variation of the reflected light as the signal, as shown in Fig. 3, where the road surface is imaged on the front of the detectors by the lenses. Hence the time histroy of detected signals can be represented as follows,

$$a_i(t)=\int_0^{L_i}\zeta_i(l_i,\ t)\ dl_i \quad (i=1\sim5), \qquad (1)$$

where, $\zeta_i(l_i,t)\ (i=1\sim5)$ are the light intensity detected at the position l_i on the i-th line detector LD_i at time t, and L_i is the length of LD_i.

On the first line detector, however, properly separated two narrow windows are provided so that it detects only the stream of the road image

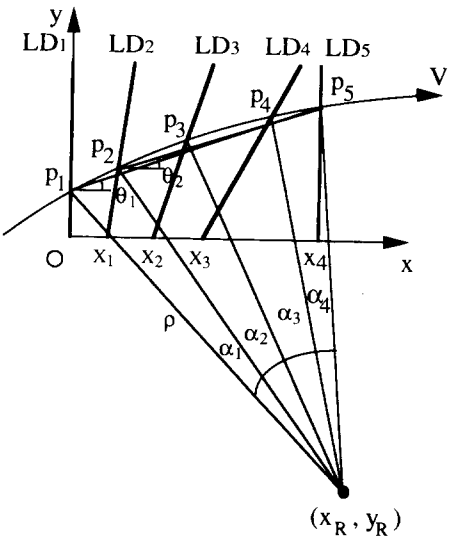

Fig. 4 Geometries between the trace and the optical line detectors

passing through these two windows. The reason of introducing these two windows will be discussed in the next section.

To explain the principle let us consider a stream of images passing through a window in the form of a circular arc with the motion parameters x_R, y_R, ρ and V, as illustrated in Fig. 4, where p_i $(i=1\sim5)$ are the cross points of the image stream and each detector, and $\alpha_i(i=1\sim4)$ are angles between the lines connecting the point p_i and the center of curvature. Then, path length of the image stream between the line detectors depend on the motion parameters and the detector's arrangement, hence inversely we can obtain information on these motion parameters from the delays of detected signals among the line detectors.

The required time delays of the image stream between the first detector and the others can be estimated by applying the fifth-order cross-correlation analysis to the five detected signals.

Here, the fifth-order moment function $m_5(\tau_1,\tau_2,\tau_3,\tau_4)$ of the detected signals is defined by

$$m_5(\tau_1,\tau_2,\tau_3,\tau_4)=\frac{1}{T}\int_0^T a_1(t)a_2(t+\tau_1)a_3(t+\tau_2)\times a_4(t+\tau_3)a_5(t+\tau_4)\ dt, \qquad (2)$$

where, T is the interval of data acquisition.

Now, let us assume that the road image patterns are sufficiently random over the road surface, hence the image stream can be represented as a random process with δ-function-like-moment function up to fifth-order ones.

Then the fifth-order moment function between the detected signals will have a peak point at the coordinates $(\tau_1, \tau_2, \tau_3, \tau_4)$ which satisfies the following relations:

$$\frac{\rho\alpha_1}{V}=\tau_1, \tag{3}$$

$$\frac{\alpha_1}{\alpha_s}=\frac{\tau_1}{\tau_4}, \tag{4}$$

$$\frac{\alpha_2}{\alpha_s}=\frac{\tau_2-\tau_1}{\tau_4}, \tag{5}$$

$$\frac{\alpha_3}{\alpha_s}=\frac{\tau_3-\tau_1}{\tau_4}, \tag{6}$$

where, $\alpha_s=\alpha_1+\alpha_2+\alpha_3+\alpha_4$.

Then, the four parameters to define the motion of the image stream can be derived from the detected delays $\tau_i(i=1,2,3,4)$ in connection with the geometry of the detectors' arrangement as follows:

$$\rho=\frac{x_4}{2\cos\theta_1\sin\left(\frac{\tau_4}{\tau_1}\Omega\right)}, \tag{7}$$

$$V=\frac{2\rho\Omega}{\tau_1}, \tag{8}$$

$$x_R=\frac{1}{2}\{x_4+\mathrm{sgn}(\rho)\tan\theta_1\sqrt{(2\rho\cos\theta_1)^2-x_4^2}\}, \tag{9}$$

$$y_R=y_1+\frac{1}{2}\{x_4\tan\theta_1-\mathrm{sgn}(\rho)\sqrt{(2\rho\cos\theta_1)^2-x_4^2}\}, \tag{10}$$

where, sgn( ) shows the sign of the arguement and y_1 is the y-coordinate of the point p_1, which is given by

$$y_1=y_3+\left(x_4-x_1+\frac{y_3}{\tan\beta}\right)\tan(\theta_1-\Omega)-x_4\tan\theta_1, \tag{11}$$

and where, y_3 is given by

$$y_3=\{x_4+2\rho\cos(\theta_1-\Omega)\sin\left(\frac{\tau_1-\tau_4}{\tau_1}\Omega\right)-x_1\}\tan\beta. \tag{12}$$

In the above relation, θ_1 and $\Omega(=\theta_1-\theta_2)$ are used as the supplementary parameters. They are shown in Fig. 4. In the derivation of ρ and V, the relations (3), (4) and $\alpha_1=2\Omega$ were used, and x_0, y_0 are derived from the geometrical relationship between θ_1, Ω, ρ and y_1. These relations can be reducd to the following two relations in terms of the two supplementary parameters θ_1 and Ω, by substituting $\alpha_i(i=1\sim4)$ represented by θ_1, Ω, ρ and y_1 into Eqs. (5) and (6):

$$\sin(\gamma+c_1\Omega)-Z_1=\tan\theta_1\{\cos(\gamma+c_1\Omega)+Z_2\}, \tag{13}$$

$$\sin(\Psi+c_2\Omega)-Z_3=\tan\theta_1\{\cos(\Psi+c_2\Omega)+Z_4\}, \tag{14}$$

where $c_1=(\tau_1+\tau_2-\tau_4)/\tau_1$, $c_2=(\tau_2+\tau_3-\tau_4)/\tau_1$ and Z_1, Z_2, Z_3, Z_4 are given by

$$Z_1=\left\{x_2-x_1+\left(\frac{\tan\beta}{\tan\gamma}-1\right)\left(x_4-x_1+x_4\cos\Omega\frac{\sin\left(\frac{\tau_1-\tau_4}{\tau_1}\Omega\right)}{\sin\left(\frac{\tau_4}{\tau_1}\Omega\right)}\right)\right\}\times\frac{\sin\left(\frac{\tau_4}{\tau_1}\Omega\right)}{\sin\left(\frac{\tau_2-\tau_1}{\tau_1}\Omega\right)}\frac{\sin\gamma}{x_4}, \tag{15}$$

$$Z_2=\left\{\left(\frac{\tan\beta}{\tan\gamma}-1\right)\left(x_4\sin\Omega\frac{\sin\left(\frac{\tau_1-\tau_4}{\tau_1}\Omega\right)}{\sin\left(\frac{\tau_4}{\tau_1}\Omega\right)}\right)\right\}\times\frac{\sin\left(\frac{\tau_4}{\tau_1}\Omega\right)}{\sin\left(\frac{\tau_2-\tau_1}{\tau_1}\Omega\right)}\frac{\sin\gamma}{x_4}, \tag{16}$$

$$Z_3=\left\{x_3-x_2+\left(\frac{\tan\gamma}{\tan\Psi}-1\right)\left(x_4-x_2+x_4\cos\Omega\frac{\sin\left(\frac{\tau_1-\tau_4}{\tau_1}\Omega\right)}{\sin\left(\frac{\tau_4}{\tau_1}\Omega\right)}\right)\right\}\left\{\left(+x_4\cos(c_1\Omega)\frac{\sin\left(\frac{\tau_2-\tau_1}{\tau_1}\Omega\right)}{\sin\left(\frac{\tau_4}{\tau_1}\Omega\right)}\right)\right\}\times\frac{\sin\left(\frac{\tau_4}{\tau_1}\Omega\right)}{\sin\left(\frac{\tau_3-\tau_2}{\tau_1}\Omega\right)}\frac{\sin\Psi}{x_4}, \tag{17}$$

$$Z_4=x_4\left\{\left(\frac{\tan\gamma}{\tan\Psi}-1\right)\left(\sin\Omega\frac{\sin\left(\frac{\tau_1-\tau_4}{\tau_1}\Omega\right)}{\sin\left(\frac{\tau_4}{\tau_1}\Omega\right)}+\sin(c_1\Omega)\frac{\sin\left(\frac{\tau_2-\tau_1}{\tau_1}\Omega\right)}{\sin\left(\frac{\tau_4}{\tau_1}\Omega\right)}\right)\right\}\times\frac{\sin\left(\frac{\tau_4}{\tau_1}\Omega\right)}{\sin\left(\frac{\tau_3-\tau_2}{\tau_1}\Omega\right)}\frac{\sin\Psi}{x_4}. \tag{18}$$

Finally, by elimination θ_1 from these relations we get

$$\sin\{\gamma+\Psi+(c_1-c_2)\Omega\}+Z_4\sin(\gamma+c_1\Omega)+Z_3\cos(\gamma+c_1\Omega)-Z_2\sin(\Psi+c_2\Omega)-Z_1\cos(\Psi+c_2\Omega)-Z_1Z_4+Z_2Z_3=0. \tag{19}$$

The solution Ω satisfying this relation corresponds to the motion parameters to be estimated. That is, by solving Eq. (19) by the proper numerical method, four parameters in Eqs. (7)~(10) can be determined, where θ_1 is determined by Eq. (13) or Eq. (14). If its solution exists near $\Omega=0$, the detected curvature will be very large and we can regard the trace of the image stream as a straight line which means that vehicle's motion is straight. the uniqueness of the solution of Eq. (19) over the region of measurable curvature limited by the size of system could be verfied although the detailes are omitted.

In this way, the required parameters to define the motion of image stream have been derived from the time delays between the detectors in connection with the geometry of detector arrangement. By the way, these parameters should be converted into the motion parameters, of the reference point of the vehicle. And, if there exists magnification in the lens system, of course, it should be taken into consider also.

Now, in the above discussions, we have considered only one image stream passing through a window. But, when two windows A and B are used as shown in Fig. 5, the fifth-order moment function of the detected signals will have two peaks and the trace of image stream passing through each window may be reconstructed one by one from the corresponding peaks observed on the fifth-order moment space.

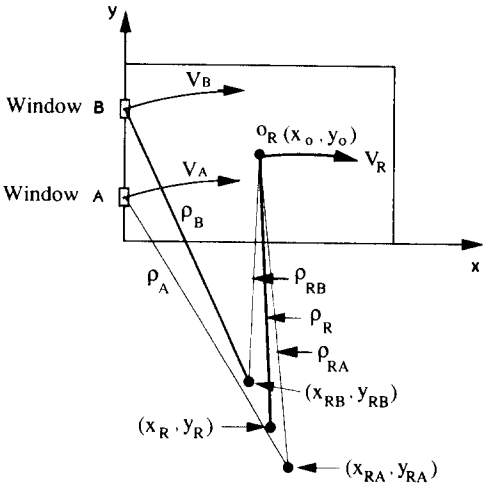

Fig. 5 Evaluation of the tracing parameters at the reference point o_R from the measured ones at two windows

The motion parameters of the reference point is estimated as the average of the motions derived from each window. That is, we get the final value of parameters as follows,

$$x_R=(x_{RA}+x_{RB})/2, \tag{20}$$
$$y_R=(y_{RA}+y_{RB})/2, \tag{21}$$
$$\rho_R=\sqrt{(x_0-x_R)^2+(y_0-y_R)^2}, \tag{22}$$
$$V_R=(V_{RA}+V_{RB})/2, \tag{23}$$

where, x_0 and y_0 are coordinates of the reference point o_R, and V_{RA} and V_{RB} are obtained from $(\rho_{RA}/\rho_A)V_A$ and $(\rho_{RB}/\rho_B)V_B$, respectively.

2.2 Necessity of windows and its effect

Line detectors detect the variation of two-dimensional flow of road image integrated over the line. The windows provided on the first line detector are used to extract one-dimensional image streams from such two-dimensional image flow. Figure 6 shows practical three types of window. (a) shows the replacement of the first line detector by a point detector in order to obtain exactly one-dimensional line image stream, but in this cace, the correlation between the signals

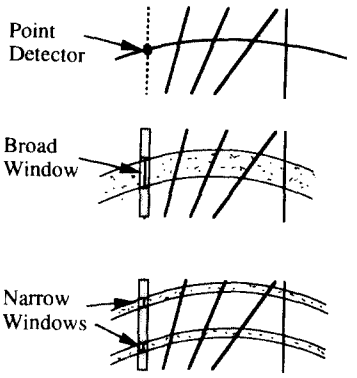

Fig. 6 Effect of employing two narrow windows instead of point detector or a broad window

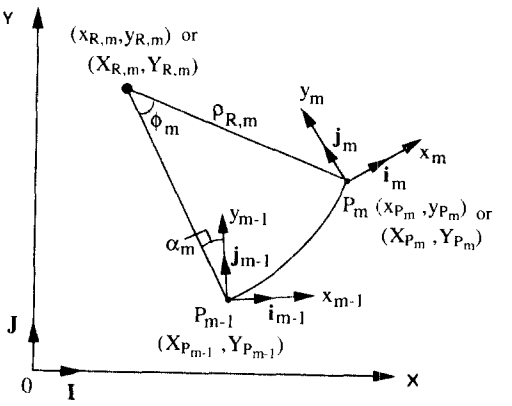

Fig. 7 Translation of the moving coordinate system x-y on the vehicle into the fixed coordinates system X-Y on the actual road

detectd by the point detector and the other line detectors will become very week. Utilization of a broad window in order to increase the correlation between the detected signals, as shown in (b), however, will reduce the spatial resolution, since the ambiguity of the peak position in the correlation space will appear. On the other hand, if we use two narrow windows separated properly as shown in (c), the degree of correlation and the accuracy of the peak detection may be maintained. From these consideration, we employed the type (c). Actually, the exact location of the image stream is estimated from the correlation analysis in our method, although it may be predetermined roughly from the arrangement of the detectors.

2.3 Reconstruction of the whole trace

For the reconstruction of the whole trace, a fixed coordinate system $X-Y$ is considered, besides the moving coordinate system $x-y$ which has its origin at the reference point of the vehicle, as are shown in Fig. 7. Subscript m means that it is determined from the data acquisited during the time interval from $(m\text{-}1)T$ to mT, where T is the measuring time interval. Thus point P_{m-1} and P_m becomes respectively the starting point and the ending point of the trace measured during the time interval between $(m\text{-}1)T$ and mT. Then the coordinates of the point P_m can be determined in the $x_{m-1}-y_{m-1}$ coordinate system as follows,

$$x_{Pm}=x_{R,m}-\rho_{R,m}\sin(\phi_m-\alpha_m), \tag{24}$$

$$y_{Pm}=y_{R,m}+\rho_{R,m}\cos(\phi_m-\alpha_m), \tag{25}$$

where ϕ_m is the turning angle and α_m is the tangential angle of the trace at point P_{m-1}, which are given by as follows,

$$\phi_m=\omega_{R,m}T=\frac{V_{R,m}}{\rho_{R,m}}T, \tag{26}$$

$$\alpha_m=\tan^{-1}\left(\frac{x_{R,m}}{y_{R,m}}\right). \tag{27}$$

Then, when we use the unit vector i_{m-1}, j_{m-1}, $\boldsymbol{I}$ and $\boldsymbol{J}$ as defined in the figure, the coordinates of the point P_m and the center of curvature can be represented in the fixed coordinate system $X-Y$ as follows,

$$X_{Pm}=X_{Pm-1}+(x_{Pm}\boldsymbol{i}_{m-1}+y_{Pm}\boldsymbol{j}_{m-1})\boldsymbol{I}, \tag{28}$$

$$Y_{R,m}=Y_{Pm-1}+(x_{R,m}\boldsymbol{i}_{m-1}+y_{R,m}\boldsymbol{j}_{m-1})\boldsymbol{J}, \tag{29}$$

$$X_{R,m}=X_{Pm-1}+(x_{R,m}\boldsymbol{i}_{m-1}+y_{R,m}\boldsymbol{j}_{m-1})\boldsymbol{I}, \tag{30}$$

$$Y_{R,m}=Y_{Pm-1}+(x_{R,m}\boldsymbol{i}_{m-1}+y_{R,m}\boldsymbol{j}_{m-1})\boldsymbol{J}. \tag{31}$$

Finally, substituting the relations between unit vectors given by

$$\boldsymbol{i}_m=T_{xx,m}\boldsymbol{I}+T_{xy,m}\boldsymbol{J}, \tag{32}$$

$$\mathbf{j}_m=T_{xy,m}\boldsymbol{I}+T_{yy,m}\boldsymbol{J}, \tag{33}$$

into Eqs. (28)~(31), we can get following new representations,

$$X_{Pm}=X_{Pm-1}+x_{Pm}T_{xx,m-1}+y_{Pm}T_{yx,m-1}, \quad (34)$$
$$Y_{Pm}=Y_{Pm-1}+x_{Pm}T_{xy,m-1}+y_{Pm}T_{yy,m-1}, \quad (35)$$
$$X_{R,m}=X_{Pm-1}+x_{R,m}T_{xx,m-1}+y_{R,m}T_{yx,m-1}, \quad (36)$$
$$Y_{R,m}=Y_{Pm-1}+x_{R,m}T_{xy,m-1}+y_{R,m}T_{yy,m-1}, \quad (37)$$

where, the components $T_{xx,m}$, $T_{xy,m}$, $T_{yx,m}$, $T_{yy,m}$ are given by

$$T_{xx,m}=\cos\phi_m T_{xx,m-1}+\sin\phi_m T_{yx,m-1}, \quad (38)$$
$$T_{xy,m}=\cos\phi_m T_{xy,m-1}+\sin\phi_m T_{yy,m-1}, \quad (39)$$
$$T_{yx,m}=-\sin\phi_m T_{xx,m-1}+\cos\phi_m T_{yx,m-1}, \quad (40)$$
$$T_{yy,m}=-\sin\phi_m T_{xy,m-1}+\cos\phi_m T_{yy,m-1}, \quad (41)$$

In this way, we can reconstruct the whole trace in the fixed coordinate system from the measured motion parameters.

3. Construction of the Optical Line Detectors

The optical line detectors were constructed by attaching optical slits, guide and photo diode array on the image plane of the camera lens system, as shown schematically in Fig. 8.

Each optical slits extracts the linear section of the image on the focal plane of the camera. The locations and the inclinations of line detectors are set as follows: $x_1=4$, $x_2=10$, $x_3=16$, $x_4=30$ (mm), and $\beta=76$, $\gamma=68$, $\Psi=62$ (degrees). The width of each slit is 0.2 mm and the vertical length was put to 20 mm. Also, on the slit corresponding to the first detector, two windows with the 2 mm length are set at the positions $y=5$ mm and $y=15$ mm, respectively.

The photo diode arrays detect the light intensity of the image passed through the corresponding slit. Each array was constructed by combining three photo diodes (Sharp BS500B). The guide was inserted between the photo diode arrays and the slits in order to reduce the unevenness of the light intensity detection sensitivity of the array due to the directivity of the photo diode.

4. Signal Processing

The outputs of three photo-diode detectors corresponding to one line detector are summed and a single detected signal is obtained for each line detector. Since the bandwidth of the detected signals was found to be less than 200 Hz for the movement of the tested object, a low pass filter with cutoff frequency of 200 Hz is also used. And detected signals are A/D converted at a sampling rate of 1 kHz, and sent to the compuder for fifth order correlation analysis. The total time

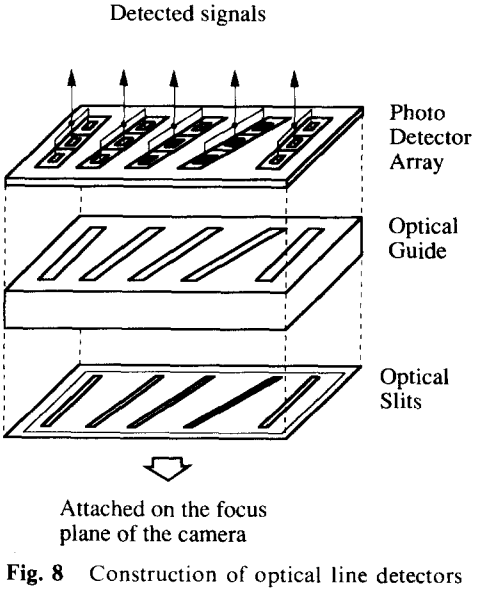

Fig. 8 Construction of optical line detectors

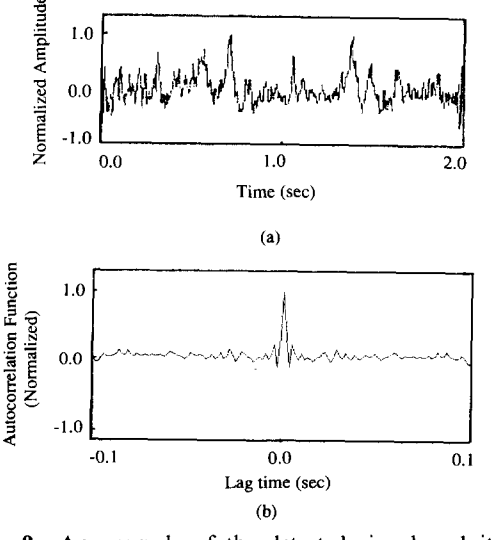

Fig. 9 An example of the detected signal and its auto-correlation function

period of data collection was about 2 sec, corresponding to the number of data of 2048.

An example of the detected signal is shown in Fig. 9, as well as its autocorrelation function. The correlation function shows a sufficiently δ-function-like form so it may confirm that the tested road has sufficiently random distribution. In the actual calculation of the moment functions, however, the signal is subtracted by the mean value and only the positive components are used.

The fifth-order cross-correlation analysis was carried out using an NEC PC9801ES personal computer that contains an i80386SX CPU. The time required for direct calculation of the fifth-order moment functions with 1024 lag points for four lag axis is extremely large, so first a series of second-order moments are calculated and positive peak positions in the fifth-order moment space are predicted from the result. That is, second-order moments function for each lag time $\tau_1 \sim \tau_4$ are first calculated and the corresponding peaks are determined. Then these peaks are used to select locations in the fifth-order moment space in which the fifth-order moment function is calculated, from which the locations with the highest and the next-to-highest peak value are selected as correct ones corresponding the windows on the first detector. The more details are omitted because this process is similar as our previous report on the measurement of the velocity field in the fluid flow (Jhang, 1989 and 1991). From these observed peak points, the parameters of motion are estimated according to the proposed propedure and the trace is reconstructed.

5. Experimental Results and Discussions

In the experiments, instead of moving the camera over the road, we moved the sham road and measured its relative movement to the fixed camera.

First, as an example of the complex movement, the turning motion was considered, and the movement of the turn-table on which the monochrome photograph of the asphalted real road

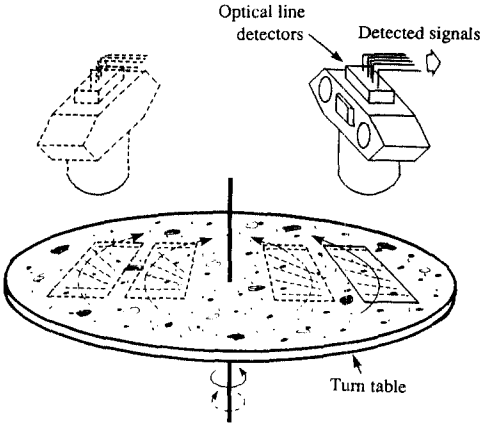

Fig. 10 First experiment using turn table

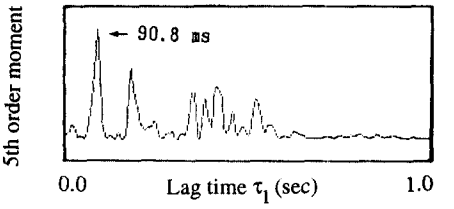

Fig. 11 A sectional view of 5th order moment function

was attached was measured, as is shown in Fig. 10, where various curvatures were prepared by changing the measuring position of the camera. Figure 11 shows one of the peak in the section of the observed fiftt-order moment funciton along lag time τ_1 which was computed for the fixed value of $\tau_2 \sim \tau_4$ at the peak point. At the selected peak point the fifth-order moment function gives peak with the highest level, hence that peak point is used as the real peak corresponding to the actual solution, while surplus peaks appeared along each axis are meaningless because they have not been predicted in the second-order correlation analysis.

Table 1 shows four examples of the results, where each of them correspond to four different measuring positions of the camera (see Fig. 10). Then, the trace was reconstructed from these estimated parameters, Fig. 12 shows an example of the whole trace reconstruction by connecting 9

Table 1 Parameter estimation results. The values in the parenthesis are the given ones

	x_R(mm)	y_R(mm)	ρ_R(mm)	ω_R(rad/s)
1	18.9	-74.1	84.2	-1.57
	(18.0)	-76.0	(86.1)	(-1.53)
2	12.1	110	-100	1.69
	(14.0)	(117)	(-107)	(1.53)
3	22.6	-34.8	45.4	-1.46
	(24.0)	(-32.0)	(43.0)	(-1.53)
4	13.5	58.8	-48.8	1.10
	(15.0)	(63.5)	(-53.5)	(0.986)

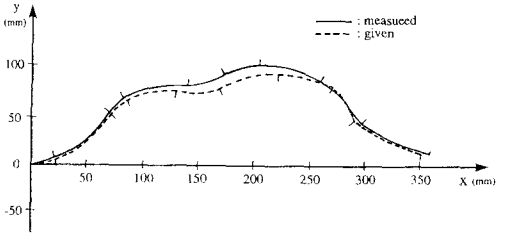

Fig. 12 Trace reconstruction result by connection nine arcs measured individually in the first experiment using turn table

traces individually measured at various camera positions and revolutions of the turn-table. The dotted line is the given trace obtained from the given parameters. The measured tace shows good agreement with the given one.

As an another example of the complex movement, the continuously moving plate was measured, as shown in Fig. 13, where the plate had been painted in black and small pieces of white paper scattered on its surface. This plate is drew putting its one side to fixed roller so that the plate moves according to the shape of the curved side. The solid line on the surface represents the trace of the reference point. Five data set with acquisition time of 2 seconds were recorded successively during the measurement, and after data acquisition the parameter estimation and the trace reconstruction were performed. Figure 14 shows the finally reconstructed trace, where the solid line is the measured trace and the dotted line is the given

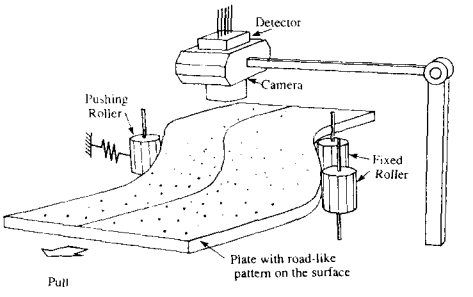

Fig. 13 Second experiment using continuously moving plate

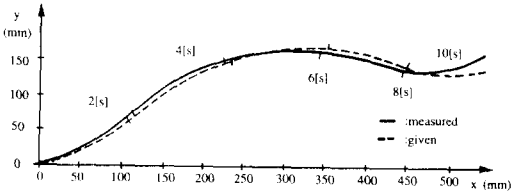

Fig. 14 Trace reconstruction result of the second experiment

one. They show good agreement each other and from above results the usefulness of our system could be confirmed.

6. Conclusion

A new method to detect the trace of comlex movement of vehicle as a set of the approximated circular arcs by using five optical line detectors and fifth-order cross-correlation analysis has been proposed. Concrete algorithms of the trace reconstruction were shown and their validity and usefulness were demonstrated by preliminary experiments using the photograph of the real road and the plate with load-like image pattern on the surface.

In the experiments, monochrome photographs of the real road and the plate with the randomly distributed white and block pattern on the surface have been used as the sham road, and their movement was measured. The results shown clearly demonstrate the usefulness of the proposed system.

The implementation of the system on to the real vehicle can be expected by realization of the real time processing hardware. Also, this method may be extended to measure more complex movement by increasing the number of the line detectors and using the corresponding high-order correlation analysis.

References

Bergh, R.A., Refevre, H.C. and Shaw, H.J., 1984, "An Overview of Fiber-Optic Gyroscopes," IEEE J. Lightwave Technol., LT-2-2, pp. 91 ~107.

Idogawa, T, Watari, M, Ohiba, R. and Takai, N., 1975 "Vehicular Speed Measurement by Correlation Techniques," Transaction of the Society of Instrument and Control Engineers, Vol. 2, No. 4, pp. 473~479 (In Japanese).

Jhang, K.Y. and Sato, T., 1989, "Flow Velocity Field Tomography Using Multiple Ultrasonic Beam Detectors and High-order Correlation Analysis," J. Acoust. Soc. Am, Vol. 86, No. 3, pp. 1047~1052.

Jhang, K.Y. and Sato, T., 1991, "3-D Velocity Field Measurement Using Multiple Ultrasonic Palne Detections and High-Order Correlation Analysis," IEEE Tr. Ultrasonics, Ferroelectrics and Frequency Control, vol. 38, No. 2, pp. 93 ~99.

Kobayashi, H., 1980, "Spatial Filter and its Applications (I)," Journal of the Society of Instrument and Control Engineers, Vol. 28, No. 1, pp. 409~417(In Japanese).

Konno, M., 1989, "Ultrasonic Gyroscope," Ultrasonic Technology, Vol. 1, No 2, pp. 67~71 (In Japanese).

Mason, W.P. and Thurston, R.N., 1979, Physical Acoustics XIV, Academic Press, New York, pp. 407~516.